Journal of Functional Materials and Applied Engineering

Research Paper

Heavy metal removal Arsenic (As) from alkaline water by modified biochar

Tom Hui[1], Sabrina Umbarila[2], Bing Wang[2], Tongji Chen[2], Rui Haller[1,*]

[1] Mexican Institute of Water Technology, Paseo Cuauhnáhuac 8532, Col. Progreso, Jiutepec, Morelos; C.P. 62550, Mexico
[2] Institute of Steel and Timber Construction, Technische Universität Dresden, 01062 Dresden, Germany
*Corresponding author:ruihaller@mailbox.tu-dresden.de

Abstract. Transformation of arsenic in the nature have been a focal point in environmental science research. Particularly in alkaline environments, the mobility and bioavailability of arsenic are relatively high, increasing the complexity of remediation. Biochar, due to its rich pore structure and good stability, is extensively used in the cleaning of heavy metal polluted water bodies. However, its ability to immobilize arsenic is limited by the electrostatic repulsion caused by its surface negative charge. Studies have shown that introducing cations can effectively enhance biochar's ability to immobilize arsenic, with calcium (Ca) being a key research focus due to its high affinity for arsenic. Nevertheless, the interaction mechanisms between biochar and arsenic with existance of calcium under alkaline conditions remain unclear, and the immobilization effects of different forms of calcium-based modified biochar need further investigation. Therefore, this study first explored the interactions between different components of biochar and arsenic in a calcium-rich system. Secondly, novel composite biochar materials were prepared by co-pyrolysis of wheat straw with different calcium-based materials. Adsorption was conducted to investigate their elimination rate for arsenic(V). Combined with material characterization, adsorption kinetics, and isotherm fitting, the key adsorption mechanisms of different biochars under Ca-rich conditions were revealed, aiming to provide a scientific basis for the efficient treatment of alkaline arsenic-contaminated wastewater. To improve the immobilization effect of biochar on arsenic(V), calcium sulfate was co-pyrolyzed with wheat straw at 800°C to prepare modified biochars with different calcium forms, labeled as SBC-800. Maximum adsorption was 861.6 mg per gram. The kinetics of adsorption followed the pseudo second order model and were controlled by intraparticle diffusion. Thermo-dynamic indicated that adsorption process of arsenic(V) by SBC-800, it was spontaneous, endothermic, and also accompanied by an increase. Mechanistic studies revealed that the removal of arsenic(V) by SBC-800 achieved efficient arsenic(V) removal through co-precipitation, complexation, redox reactions, and pore filling.

Keywords: *Biochar, Calcium Sulfate, arsenic, Removal*

Received on 24 June 2024, Accepted on 10 August 2024, Published on 15 September 2024

1 Introduction

Arsenic (As) is a metalloid located in Group VA, Period 4 of the periodic table, with atomic weight of 74.92 and an electron configuration of $4s^2 3d^{10} 4p^3$. It has a bright silvery-gray appearance. Arsenic is widely distributed in nature, with an average crustal abundance of about 2.5 $mg \cdot kg^{-1}$. Arsenic (As) exists in the water bodies of nature environment in both inorganic and organic nature, its toxicity changing significantly depending on the species. Inorganic arsenic primarily includes arsenic(V), arsenic(III), and metallic; organic arsenic often exists as compounds such as monomethylarsonic acid (MMA) and dimethylarsinic acid (DMA) [1]. In comparison, inorganic arsenic is far more toxic than organic arsenic, with arsenic(III) being over 60 times more toxic than arsenic(V) due to its higher reactivity towards biomolecules [2]. Methylated arsenic species like MMA and DMA have moderate toxicity, while other organic forms are generally considered non-toxic [3]. In aqueous solutions, arsenic(III) and arsenic(V), due to their high charge and small ionic radii, primarily exist as oxyanions [4]. The distribution and speciation of arsenic compounds in hydrological systems are significantly effectd by redox potential and pH [5]. For example, in environments with high redox potential, arsenic tends to exist stably as arsenic(V), such as $H_3 arsenic O_4$, $H_2 arsenic O_4^-$, $H arsenic O_4^{2-}$, or $arsenic O_4^{3-}$; under reducing conditions with low

redox potential and acidic or weakly alkaline pH, arsenic(III) predominantly exists as the uncharged $H_3arsenicO_3$ molecule.

Currently, arsenic sources are mainly derived from natural processes and anthropogenic activities. Natural arsenic (As) sources are closely related to various geological and biological processes, such as rock weathering, microbial activity, and volcanic eruptions. arsenic often deposits in sedimentary rocks, volcanic rocks, and soils as sulfides [6]. Anthropogenic activities are significant supplementary sources of arsenic distribution, including mining operations, fossil fuel combustion, application of arsenic-containing pesticides and herbicides, production of crop desiccants, and the use of arsenic compounds as additives in livestock feed (especially in poultry farming). Furthermore, the alkaline treatment of arsenic-containing solid waste is a key method for selectively recovering valuable metals from non-ferrous metal smelting processes [7]. Alkaline leaching of some arsenic-bearing slags containing carbonate can generate typical high-salinity alkaline arsenic-containing wastewater, with leachates often containing large amounts of sodium arsenate (Na_3AsO_4) and sodium carbonate (Na_2CO_3).

Adsorption is efficient for arsenic removal because of its efficiency, operational simplicity, and selectivity. The effectiveness of adsorption depends heavily on the choice of adsorbent. Common effective adsorbents include activated alumina [8], activated carbon [9], manganese dioxide [10], iron hydroxide [11], zeolite [12], clay [13], zero-valent iron [14], and biomass materials [15]. These adsorbents are often favored due to their wide availability, low cost, large amount of surface active sites, huge specific surface area, and strong regeneration capacity. However, the adsorption method, its efficiency is primarily determined by the composition and type of adsorbent. Additionally, factors such as temperature, pH, and the existance of interfering ions can easily affect the process of adsorption.

Despite its advantages, existing industrial adsorbents are often costly, hindering large-scale application. Therefore, developing low-cost, readily available, and efficient adsorption materials has become a key research direction for managing arsenic contamination in water bodies. Biochar, with its abundant raw materials, developed pore structure, complex surface morphology, and numerous functional groups that contain oxygen (e.g., carboxyl, hydroxyl, amino) and inorganic elements, exhibits strong adsorption capacity for heavy metals and is considered a highly promising adsorbent.

In recent years, arsenic contamination in water bodies has become increasingly severe, especially in alkaline environments where arsenic's activity and mobility are enhanced, complicating remediation efforts. Adsorption is a common remediation method, and developing low-cost, efficient adsorbents is crucial. Biochar, with its unique physicochemical properties, can effectively remove heavy metals from water, showing broad application prospects in water pollution control [5]. However, because biochar typically carries a negative surface charge, electrostatic repulsion with arsenic oxyanions reduces its arsenic elimination rate. Thus, modifying biochar is necessary to enhance its performance. Calcium-based materials, due to their high affinity for arsenic(V), can be used to modify biochar and improve its arsenic removal capability. Furthermore, different components of biochar interact with arsenic through different mechanisms, and the effect of calcium ions (Ca^{2+}) in the environment on the interaction between biochar and arsenic is not yet clear. Elucidating the interaction mechanisms of biochar's soluble and insoluble components with arsenic in the presence of Ca^{2+} can provide a foundation for the application and modification of calcium-based biochar [10]. However, systematic studies on the immobilization of arsenic by different biochar components in alkaline environments and research on biochar modified with different types of calcium-based materials are still relatively scarce.

Therefore, addressing the issue of low arsenic(V) elimination rate by biochar in alkaline environments, this study first investigated the interaction mechanisms between different biochar components and arsenic(V) in a calcium enriched system. Secondly, novel calcium-based composite biochars were prepared by co-pyrolysis of wheat straw with different calcium-based materials. Their arsenic(V) removal performance was systematically evaluated through batch adsorption experiments. Combined with material characterization, adsorption kinetics, and isotherm model analysis, the key adsorption mechanisms of different types of biochar under Ca-rich conditions were elucidated.

2 Materials and Methods

2.1 Preparation process of Biochar

Screened wheat straw powder was uniformly mixed with calcium sulfate powder at a weight ratio of 1:1. The mixture was heated in a tube furnace in a N_2 atmosphere at a heating rate of 20 °C/min to the target temperatures of 800 °C and held for 2 hours. After that, the material was cooled to room temperature, ground using an agate mortar, and sieved through a 200-mesh sieve to obtain uniform biochar products. The final products, defined as SBC 800, were stored in sealed containers to prevent moisture.

2.2 Batch Adsorption Experiments

As(V) solutions with different concentrations (range 0-1000 mg/L) were prepared. The initial pH of the As(V) solutions was adjusted to 11.0 ± 0.1 using 1 mol/L HCl or NaOH. In brief, 0.1 g of adsorbent was uniformly mixed with the different concentrations of As(V) solution and stirred at room temperature for 24 hours using a multi-point magnetic stirrer. The mixture after adsorption equilibrium was filtered, and the supernatant was collected and stored in centrifuge tubes. The concentration of As(V) in the supernatant was determined to evaluste the adsorption performance of the biochar for As(V).

As(V) solution was prepared (800 mg/L). The initial pH of the solutions was adjusted to 11.0 ± 0.1. 0.1 g of adsorbent was fully mixed with the solution in a 100 mL beaker and placed on a multi-point magnetic stirrer for the adsorption experiment. Samples were taken at different contact times (10-1440 min), and the concentration of As(V) in the filtrate was measured to calculate the adsorption capacity (q_t) of the biochar for arsenic(V) at time t.

At room temperature, 0.1 g of char was added to 100 mL of As(V) solution (concentration reference from kinetic experiments) in a 100 mL beaker. The initial pH of the solution was adjusted to 7.0 ± 0.1, 8.0 ± 0.1, 9.0 ± 0.1, 10.0 ± 0.1, 11.0 ± 0.1, and 12.0 ± 0.1, respectively. The effect of different alkaline environments on the adsorption efficiency of As(V) by the adsorbent was investigated, and the adsorption capacity was estimated.

A certain concentration of As(V) solution was prepared, and interfering ions (SO_4^{2-}, HCO_3^-, NO_3^-, Cl^-, $H_2PO_4^-$) at concentrations of 0.01 mol/L and 0.1 mol/L were added separately to simulate real wastewater. The adsorbent dosage was set at 0.1 g, and the solution pH was adjusted to 11.0 ± 0.1. The biochar and 100 mL of the mixed solution were added to a 100 mL beaker. The effect of these interfering ions on the adsorption efficiency of arsenate by the adsorbent in aqueous solution was investigated, and the adsorption capacity for As(V) was evaluated.

2.3 Analytical Methods

2.3.1 Analysis of Target Pollutant Concentration

Total arsenic was determined as follows: 5 mL of filtered reaction solution was placed in a 25 mL colorimetric tube. 0.1 mL of 11% hydrochloric acid solution and 0.1 mL of 2 mmol/L potassium iodate solution were added. After shaking and standing for 1 hour, arsenic(III) in the solution was oxidized to arsenic(V). Then, 0.8 mL of prepared molybdenum antimony reagent and 1 mililiter of freshly prepared As acid solution were added, and the volume was prepared to 10 mL with deionized water. After standing at temperature of 20 °C for 1 hour, the As concentration was measured at a wavelength of 870 nm using the spectrophotometer, with a blank experiment conducted simultaneously. After measuring the absorbance, a standard curve was constructed, and the corresponding sample concentration was determined from the absorbance value on the standard curve.

Determination of arsenic(V) Concentration in Samples was carried out as follows: The procedure was the same as for total arsenic determination, except that the 11% hydrochloric acid and potassium iodate solutions were not added. The concentration of arsenic(III) was calculated as the difference between total arsenic and arsenic(V). The concentration of Ca^{2+} in this experiment was determined using flame atomic absorption spectrometry.

2.3.2 Material Characterization

XRD was performed for phase analysis and crystallinity determination using a Bruker D8 Advance X-ray diffractometer (Germany). The experiment used a Cu Kα radiation source (λ = 0.15418 nm), with operating voltage and current set at40 mA and 40 kV , respectively. The scanning mode was continuous step scanning with a speed of 15°·min^{-1}, step size of 0.03°, and the diffraction angle (2θ) scanning range set from 3° to 85°.

Functional groups of the materials surface were detected using a PerkinElmer Spectrum Two Fourier Transform Infrared Spectroscopy (FTIR) spectrometer (USA). Samples were prepared using the potassium bromide pellet method, and full-spectrum scanning was performed in the wavenumber ranging from 4000to 400 cm^{-1}.

4. Results and Discussion

4.1 Isothermal Adsorption of As(V) by Calcium Sulfate Modified Biochar

To evaluate the adsorption performance of $CaSO_4$ modified biochar under different initial arsenic(V) concentrations, this study systematically investigated effect of starting arsenic(V) concentration on adsorption behavior. Results showed that, SBC-800 exhibited superior adsorption performance across the entire concentration range. Its adsorption capacity increased markedly with rising initial As(V) concentration, especially under high concentration conditions. When the initial concentration reached 800 mg/L, the adsorption capacity of SBC-800 approached saturation, with a maximum value as high as 753.8 mg/g(Figure 1), demonstrating its strong adsorption capability for As(V).

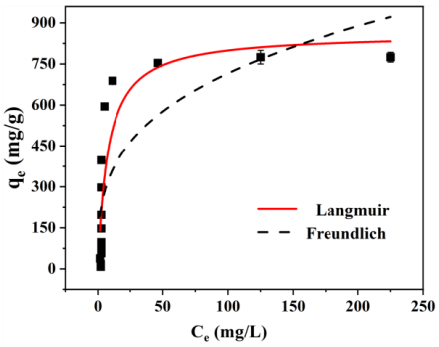

Figure 1 Isothermal fitting curves of arsenic(V) by SBC-800

The Freundlich as well as Langmuir classical isothermal adsorption behavior were used to fit the arsenic(V) adsorption behavior of SBC-800 under different initial concentrations. The results showed that, for SBC-800, the Langmuir model provided a better fitting, with an R^2 of 0.7959, indicating that its adsorption behavior was predominantly monolayer adsorption [16]. The Freundlich model yielded a poor fit with an R^2 of only 0.6374, suggesting that although some multilayer adsorption characteristics might exist, the overall process mainly followed a monolayer mechanism. From a mechanistic perspective, the Langmuir model corresponding to monolayer adsorption is primarily controlled by hydrogen bonding interactions as well as precipitation, while the Freundlich model involves electrostatic-interactions and also van der Waals forces [17].

4.2 Kinetics of arsenic(V) Adsorption by Calcium Sulfate Modified Biochar

As shown in Figure 2, during the initial stage of adsorption (time < 60 min), the adsorption capacity of SBC-800 for arsenic(V) increased rapidly with time, from 0 to 672.5 mg·g^{-1}, indicating high adsorption efficiency in the early stage for both materials. This significant initial adsorption is mainly attributed to the abundant active sites and vacancies on the material surface, providing ample binding positions for arsenic(V) ions. arsenic the reaction time prolonged, the adsorption rate gradually slowed down. SBC-800 reached equilibrium at 240 min with an adsorption capacity of 751.3 mg·g^{-1}. The decrease in adsorption rate indicates that after arsenic(V) rapidly occupied the active sites initially, the process gradually transitioned to a slower stage as available sites diminished, possibly limited by diffusion rates and internal surface sites [18].

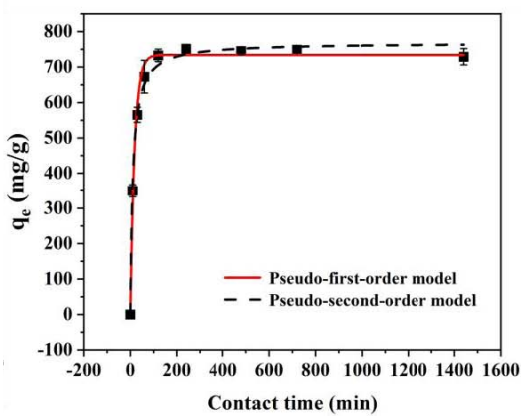

Figure 2 Kinetic fitting curves of arsenic(V) by SBC-800

To further analyze the As(V) adsorption kinetics of on SBC-800, the pseudo-first-order, and pseudo-second-order, were fitted to the experimental data. The results showed that, the pseudo-second-order model provided a better fitting for biochar material compared to the first-order model. The correlation coefficients for SBC-800 was 0.9921 (pseudo-first-order) and 0.9941 (pseudo-second-order), respectively, indicating that the adsorption processes for both were primarily controlled by chemical adsorption mechanisms.

4.3 Effect of pH on arsenic(V) Adsorption by Calcium Sulfate Modified Biochar

The experimental results on the effect of pH value on the As(V) adsorption performance of calcium sulfate modified biochar are shown in Figure 3. The results indicate that, when the pH value of the SBC-800 system increased from 7 to 9, its adsorption capacity for As(V) enhanced. As the pH increasing further from 9 to 12, the adsorption ability of SBC-800 decreased. The initial increase might be because higher pH conditions favor the formation of Ca-arsenic precipitates, thereby improving adsorption efficiency. The subsequent decrease might be related to competitive adsorption effects caused by excessively high OH^- concentrations [19, 20]. Overall, although pH changes affected the adsorption efficiency to some extent, the impact on the overall arsenic(V) adsorption by SBC-800 was relatively limited.

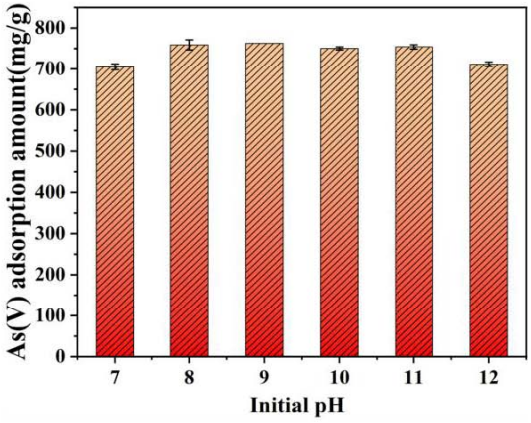

Figure 3 Effect of initial pH on arsenic(V) adsorption by SBC-800

4.4 Effect of Interfering Ions on arsenic(V) Adsorption by Calcium Sulfate Modified Biochar

Anions commonly present in water bodies and wastewater (such as $H_2PO_4^-$, NO_3^-, Cl^-, etc.) may compete with arsenic(V) for active-sites on the adsorbent-surface, thus affecting the elimination rate of arsenic(V). In this study, effect of different interfering anions on the arsenic(V) adsorption process was systematically investigated, and the results are shown in Figure 4.

Compared to the control experiment without interfering ions,Notably, at lower concentrations (0.01 mol/L) of Cl^- and NO_3^-, these monovalent anions promoted arsenic(V) adsorption to some extent. This phenomenon might be attributed to the weak competitive adsorption ability of Cl^- and NO_3^- ions, preventing them from effectively occupying adsorption sites. Instead, at low concentrations, they might slightly increase arsenic(V) adsorption capacity through an ionic strength effect. However, when the concentrations of Cl^- and NO_3^- increased further, the competitive effect gradually dominated, leading to a decrease in arsenic(V) adsorption capacity [21].

In the SBC-800 system, the presence of various anions (Cl^- and NO_3^-) in the SBC-800 system reduced the removal capacity of SBC-800 for arsenic(V) to varying degrees. This inhibitory effect became more pronounced with increasing concentration of the interfering anions, indicating that anions not only compete with arsenic(V) for adsorption sites but may also affect other key factors in the adsorption process. Under strong alkaline conditions, arsenic(V) primarily exists as arsenicO_4^{3-}, and the adsorbent surface may be negatively charged [22]. The addition of external anions significantly enhances the electrostatic repulsion effect, thereby inhibiting the effective adsorption of arsenicO_4^{3-} on the material surface. Interfering anions might also reduce arsenic(V) adsorption efficiency by competing with active sites on the adsorbent surface or with Ca^{2+} in the system. Even at higher concentrations (0.1 mol/L), the effect of these ions remained limited. This phenomenon might be because SBC-800 can release more free Ca, and Ca-arsenic precipitation is the primary fixation form. The competition and electrostatic repulsion from these ions cannot overly affect the adsorption of that by SBC-800.

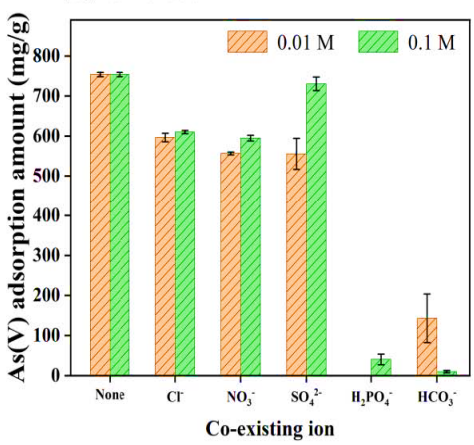

Figure 4 Effect of interfering ions on arsenic(V) adsorption by SBC-800

Among all the tested interfering anions, $H_2PO_4^-$ and HCO_3^- had the most significant inhibitory effect on arsenic(V) adsorption by SBC-800. In the presence of $H_2PO_4^-$ and HCO_3^-, the adsorption capacity decreased from 753.8 mg/g to a minimum of 0 mg/g and 10.0 mg/g for SBC-800, respectively. This significant decline is closely related to the competition mechanism between arsenicO_4^{3-} and other anions. Firstly, phosphorus and arsenic belong to the same group (Group VA) in the periodic table, so arsenate and phosphate share high similarity in chemical structure and properties. arsenic(V) mainly exists as HarsenicO_4^{2-} or arsenicO_4^{3-}, which are highly similar to $H_2PO_4^-$ in molecular structure and spatial configuration, both being tetrahedral oxyanions [22]. Additionally, both anions possess strong nucleophilicity and tend to compete for metal active sites (e.g., Ca^{2+}) on the adsorbent surface. Since the ionic radius of P is smaller than that of arsenic, phosphate ions at high concentrations may preferentially occupy the adsorption sites on the material surface, directly hindering the effective adsorption of arsenic(V). The strong inhibitory effect of HCO_3^- on arsenic(V) adsorption operates through a different mechanism compared to $H_2PO_4^-$. This inhibition may stem from two aspects: On one hand, HCO_3^-, as a buffering ion, tends to react with H^+ under strong alkaline conditions to form CO_3^{2-} or regulate the local pH of the solution through carbonate equilibrium [23]. An increase in pH might alter the speciation of arsenic(V), thereby affecting its adsorption behavior on the SBC-800 surface. For example, at higher pH, arsenic(V) tends to exist more as arsenicO_4^{3-}, which, with its higher negative charge, might experience stronger electrostatic repulsion with the potentially charged material surface, leading to reduced adsorption capacity. On the other hand, HCO_3^- might also interact with active sites on the adsorbent surface, forming $CaCO_3$ precipitate, or form soluble complexes with arsenic(V) [24]. These processes not only consume adsorption sites but may also

reduce adsorption efficiency by covering or passivating the material surface.

4.5 Mechanism of arsenic(V) Adsorption by Calcium Sulfate Modified Biochar

The XRD patterns of SBC-800 before or after arsenic(V) adsorption are illustrated in Figure 5a. Before adsorption, the XRD pattern of SBC-800 showed that it primarily contained highly crystalline CaS, with no other calcium-based minerals detected, indicating that the material retained the calcium sulfide structure during the heat treatment process. After arsenic(V) adsorption, the diffraction peaks for CaS vanished. Simultaneously, characteristic peaks for arsenicS appeared at 15.4°, suggesting that arsenic(V) may have reacted with S^{2-} to form an arsenic-S type precipitate. Furthermore, characteristic diffraction peaks for $Ca_3(arsenicO_4)_2$ and $Ca_5(arsenicO_4)_3(OH)$ also appeared in the pattern, providing further verification of the chemical precipitation reaction between Ca^{2+} and $arsenicO_4^{3-}$, which is a key mechanism supporting arsenic(V) removal. It is noteworthy that diffraction peaks for $CaCO_3$ were also detected in the samples after adsorption. These likely originated from the precipitation of calcium carbonate formed by the reaction of dissolved CO_2 with free Ca^{2+} under alkaline conditions, consequently affecting the final mineral composition of the material [25].

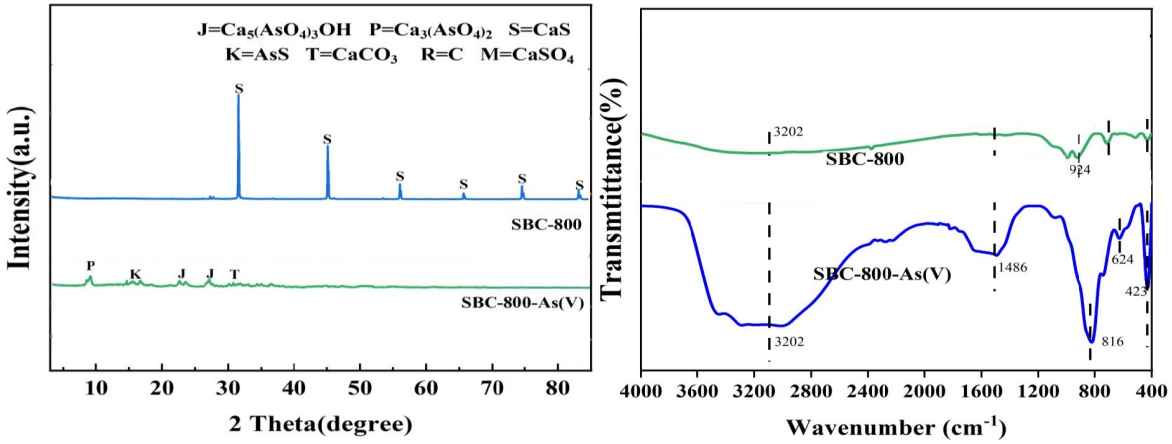

Figure 5 XRD patterns of SBC-800 (a); FTIR spectra ofSBC-800 before and after arsenic(V) adsorption (b)

The FTIR spectra of SBC-450 and SBC-800 before or after arsenic(V) adsorption are shown in Figure 5b. Overall, it exhibited characteristics typical of inorganic minerals and oxygen-containing functional groups before adsorption. Prior to adsorption, a broad -OH stretching vibration absorption band was observed in the range of 3600-3000 cm^{-1} for both materials. After adsorption, the intensity of the -OH peak increased in both materials. The change observed at 3202 cm^{-1} might be attributed to the formation of $Ca_5(arsenicO_4)_3(OH)$, indicating a precipitation reaction between arsenic(V) and Ca^{2+} [26].

In the mid-infrared region, the strong absorption band centered at 1140 cm^{-1} in SBC-450 before adsorption split into peaks at 1151 cm^{-1}, 668 cm^{-1}, and 597 cm^{-1} after adsorption. The peaks at 706 cm^{-1} and 403 cm^{-1} are attributed to Ca-S and Ca-O stretching vibrations, respectively, indicating that CaS is the primary mineral phase. After arsenic(V) adsorption, these characteristic peaks disappeared. Coupled with the appearance of new arsenic-O vibration peaks at 803 cm^{-1} and 816 cm^{-1}, this indicates that the adsorption process involved significant mineral transformation and chemical reactions, potentially forming low-solubility precipitates such as arsenic-S complexes, $Ca_3(arsenicO_4)_2$, and $Ca_5(arsenicO_4)_3(OH)$ [27].

Furthermore, after adsorption, characteristic vibration peaks for CO_3^{2-} appeared in the range of 1411-1486 cm^{-1} for both materials. It is speculated that CO_2 reacted with Ca^{2+} under alkaline conditions during adsorption, forming $CaCO_3$ precipitate, which further altered the surface mineral composition of the materials. Notably, the peaks present at around 924 cm^{-1} before adsorption in SBC-800, associated with C-O-C, C-OH, and C-O-vibrations, disappeared after adsorption. This suggests that these functional groups that contain oxygen may have participated in the complexation process with arsenic(V).

Conclusion

In this work, the adsorption performance of $CaSO_4$ modified biochar (BC-800) on as (V) was mainly explored, and the optimal adsorption conditions were determined. At the same time, the adsorption kinetics and/or isotherm model fitting analysis of the adsorption process of SBC-800 for as (V) were carried out, and the morphological characteristics, crystal structure, surface functional groups and surface element valence changes of the modified biochar before and after adsorption were analyzed to explore its potential mechanism. The main conclusions resulted from analysis are listed as follows:

The fitting results of isothermal adsorption experiments dispalyed that the adsorption process of SBC-800 for As (V) conformed to Langmuir isothermal adsorption equation, and its adsorption belonged to uniform monolayer adsorption. The fitting results for kinetic of adsorption experiments showed that the adsorption of as (V) by SBC-800 reached equilibrium at 240 min, which conformed to the quasi second-order kinetic model. It was controlled by chemical reaction, and the intra particle diffusion was probably the main controlling factor of adsorption rate in the adsorption process. In thermodynamic experiments, the adsorption of as (V) by SBC-800 was spontaneous, endothermic and entropy increasing. In the effect experiment of initial pH value, with the increase of pH value, the adsorption ability first increased and then decreased. In the adsorption experiment of interfering ions, each anion has different degrees of inhibition on the adsorption behaviour of as (V).

Through batch experiments of adsorption, as well as characterization before and after adsorption, the results illustrated thatthe adsorption mechanism of SBC-800 for as (V) was mainly coprecipitation, oxidation-reduction, complexation and pore filling.

References

[1] CANTRELL K B, HUNT P G, UCHIMIYA M, et al. Impact of pyrolysis temperature and manuresource on phys icochemical characteristics of biochar[J]. Bioresource Technology, 2012, 107: 419-428.

[2] RONSSE F, VAN HECKE S, DICKINSON D, et al. Production and characterization of slow pyrolysis biochar: e ffect of feedstock type and pyrolysis conditions[J]. GCB Bioenergy, 2013, 5(2): 104-115.

[3] YANG F, XU Z, YU L, et al. Kaolinite enhances the stability of the dissolvable and undissolvable fractions of biochar via different mechanisms[J]. Environmental Science & Technology, 2018, 52(15): 8321-8329.

[4] ZHONG D, ZHAO Z, JIANG Y, et al. Contrasting abiotic arsenic(III) immobilization by undissolved and dissol ved fractions of biochar in Ca2+-rich groundwater under anoxic conditions[J]. Water Research, 2020, 183: 116106.

[5] DONG X, MA L Q, GRESS J, et al. Enhanced Cr(VI) reduction and arsenic(III) oxidation in ice phase: importa nt role of dissolved organic matter from biochar[J]. Journal of Hazardous Materials, 2014, 267: 62-70.

[6] CHEN N, HUANG Y, HOU X, et al. Photochemistry of Hydrochar: Reactive Oxygen Species Generation and S ulfadimidine Degradation[J]. Environmental Science & Technology, 2017, 51(19): 11278-11287.

[7] ZHONG D, ZHANG Y, WANG L, et al. Mechanistic insights into adsorption and reduction of hexavalent chro mium from water using magnetic biochar composite: key roles of Fe3O4 and persistent free radicals[J]. En vironmental Pollution, 2018, 243: 1302-1309.

[8] ZHONG D, JIANG Y, ZHAO Z, et al. pH dependence of arsenic oxidation by rice-husk-derived biochar: roles of redox-active moieties[J]. Environmental Science & Technology, 2019, 53(15): 9034-9044.

[9] HAN Y S, PARK J H, KIM S J, et al. Redox transformation of soil minerals and arsenic in arsenic-contaminat ed soil under cycling redox conditions[J]. Journal of Hazardous Materials,

[10] 2019, 378: 120745.

[11] HUSSAIN M M, BIBI I, NIAZI N K, et al. arsenic biogeochemical cycling in paddy soil-rice system: interaction with various factors, amendments and mineral nutrients[J]. Science of the Total Environment, 2021, 773: 145040.

[12] LUO T, SUN J X, LIU ,Y, et al. Adsorption and transport behavior of arsenate on saline-alkali soils of tidal fla t of yellow sea, eastern China[J]. Environmental Pollutants and Bioavailability, 2019, 31(1): 166-173.

[13] ALCHOURON J, NAVARATHNA C, RODRIGO P M, et al. Household arsenic contaminated water treatment e mploying iron oxide/bamboo biochar composite: an approach to technology transfer[J]. Journal of Colloid and Interface Science, 2021, 587: 767-779.

[14] ZAMA E F, LI G, TANG Y T, et al. The removal of arsenic from solution through biochar enhanced precipitat ion of calcium-arsenic derivatives[J]. Environmental Pollution, 2022, 292: 118241.
[15] NEKHUNGUNI P M, TAVENGWA N T, TUTU H. Investigation of arsenic(V) removal from acid mine drainage by iron (hydr) oxide modified zeolite[J]. Journal of Environmental Management, 2017, 197: 550-558.
[16] OZOLA R, KRAUKLIS A, LEITIETIS M, et al. FeOOH-modified clay sorbents for arsenic removal from aqueou s solutions[J]. Environmental Technology & Innovation, 2019, 13: 364-372.
[17] WANG Y, ZHANG X, JU N, et al. High capacity adsorption of antimony in biomass-based composite and its consequential utilization as battery anode[J]. Journal of Environmental Sciences, 2023, 126: 211-221.
[18] JIAO P, DELUCA T H, WANG K, et al. Fire-deposited charcoal enhances soil microbial biomass in a recently harvested subtropical plantation forest[J]. Geoderma, 2024, 448: 116964.
[19] SHIRVANIMOGHADDAM K, CZECH B, ABDIKHEIBARI S, et al. Microwave synthesis of biochar for environm ental applications[J]. Journal of Analytical and Applied Pyrolysis, 2022, 161: 105415.
[20] HUEZO L, VASCO-CORREA J, SHAH A. Hydrothermal carbonization of anaerobically digested sewage sludg e for hydrochar production[J]. Bioresource Technology Reports, 2021, 15: 100795.
[21] SHAH A, DARR M J, DALLUGE D, et al. Physicochemical properties of bio-oil and biochar produced by fast pyrolysis of stored single-pass corn stover and cobs[J]. Bioresource Technology, 2012, 125: 348-352.
[22] EBADOLLAHZADEH H, ZABIHI M. Competitive adsorption of methylene blue and Pb (II) ions on the nano-m agnetic activated carbon and alumina[J]. Materials Chemistry and Physics, 2020, 248: 122893.
[23] HUNG D Q, NEKRASSOVA O, COMPTON R G. Analytical methods for inorganic arsenic in water: a review[J]. Talanta, 2004, 64(2): 269-277.
[24] SEVAK P, PUSHKAR B. arsenic pollution cycle, toxicity and sustainable remediation technologies: a compre hensive review and bibliometric analysis[J]. Journal of Environmental Management, 2024, 349: 119504.
[25] ASHFAQ M Y, AL-GHOUTI M A, DA'NA D A, et al. Investigating the effect of temperature on calcium sulfat e scaling of reverse osmosis membranes using FTIR, SEM-EDX and multivariate analysis[J]. Science of the Total Environment, 2020, 703: 134726.
[26] LIU X, LV J. Efficient phosphate removal from wastewater by Ca-laden biochar composites prepared from eggshell and peanut shells: a comparison of methods[J]. Sustainability, 2023, 15(3): 1778.
[27] YANG J, ZHANG M, WANG H, et al. Efficient recovery of phosphate from aqueous solution using biochar d erived from co-pyrolysis of sewage sludge with eggshell[J]. Journal of Environmental Chemical Engineerin g, 2021, 9(5): 105354.